

1  
2  
3  
4  
5  
6  
7  
8  
9  
10  
11  
12  
13  
14  
15  
16  
17  
18  
19  
20  
  
21  
  
22  
  
23  
24

## **A retinal model of cerebral malaria**

François Paquet-Durand<sup>1&\*</sup>, Susanne C. Beck<sup>2&</sup>, Soumyaparna Das<sup>1</sup>, Gesine Huber<sup>2</sup>, Le Chang<sup>3,4</sup>, Timm Schubert<sup>3,4</sup>, Naoyuki Tanimoto<sup>2</sup>, Marina Garcia-Garrido<sup>2</sup>, Regine Mühlfriedel<sup>2</sup>, Sylvia Bolz<sup>3</sup>, Wolfgang Hoffmann<sup>5</sup>, Ulrich Schraermeyer<sup>6</sup>, Benjamin Mordmüller<sup>5</sup>, Mathias Seeliger<sup>2</sup>

<sup>1</sup> Cell Death Mechanisms Lab, Institute for Ophthalmic Research, University of Tübingen, Germany.

<sup>2</sup> Division of Ocular Neurodegeneration, Institute for Ophthalmic Research, University of Tübingen, Germany.

<sup>3</sup> Institute for Ophthalmic Research, University of Tübingen, Germany.

<sup>4</sup> Centre for Integrative Neuroscience (CIN), University of Tübingen, Germany.

<sup>5</sup> Institute for Tropical Medicine, University of Tübingen, Germany.

<sup>6</sup> Experimental Vitreoretinal Surgery, Institute for Ophthalmic Research, University of Tübingen, Germany.

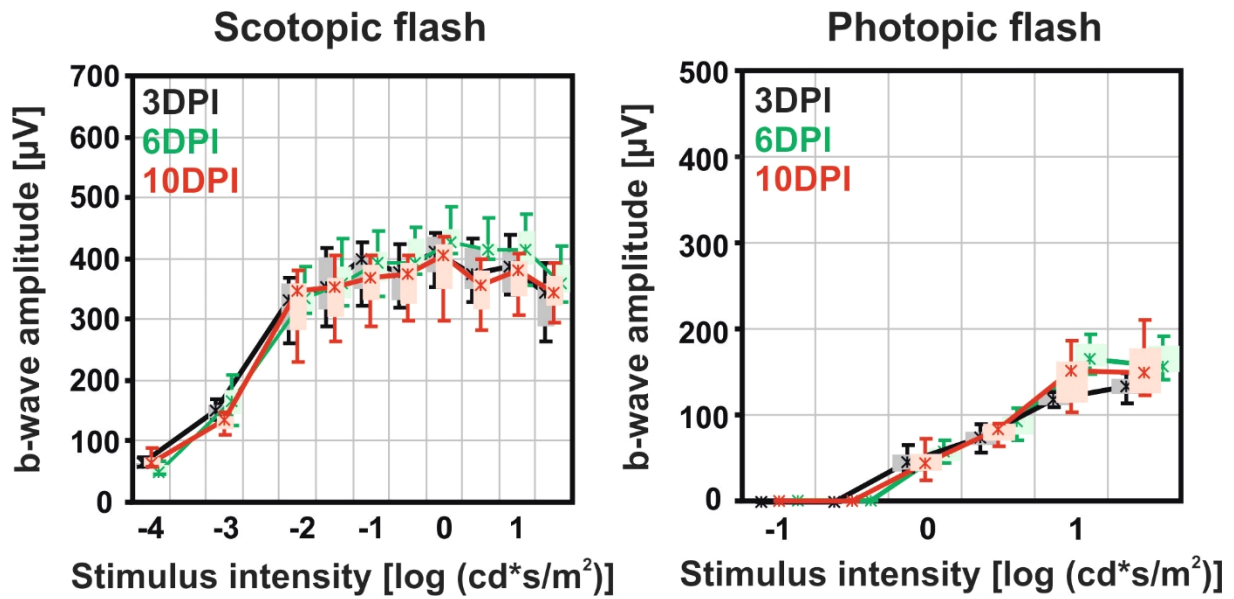
\* Corresponding Author

E-Mail: francois.paquet-durand@klinikum.uni-tuebingen.de

& These authors contributed equally to this work

## **Supplementary figures and captions**

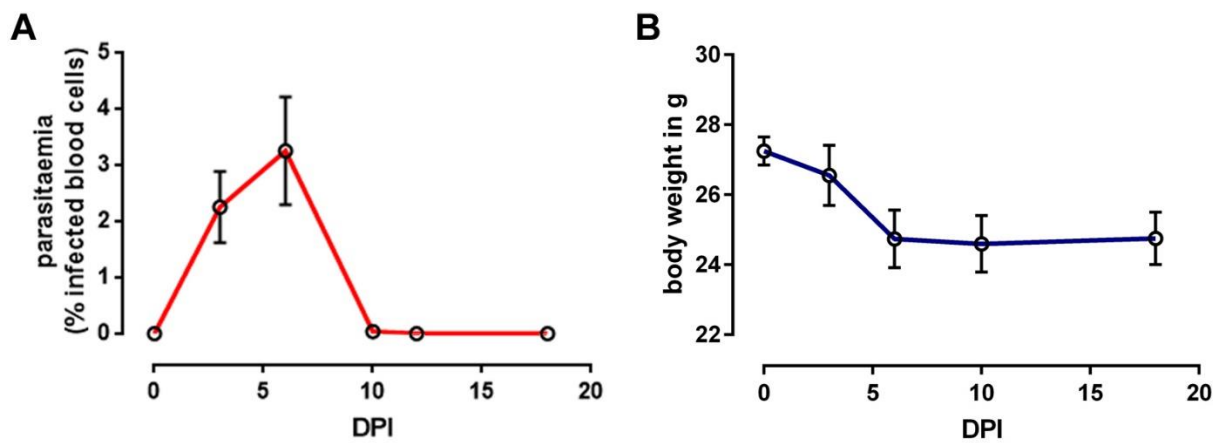
25



26

27 **Fig. S1: Functional analysis of the retina during infection.** No alterations of the retinal  
28 function at 3, 6, and 10DPI (*i.e.* 4 days post treatment), respectively, could be observed in the  
29 quantitative evaluation (box-and-whisker plot) of the scotopic (A, left) and photopic (B) b-wave  
30 amplitudes (n=4). Boxes indicate 25% and 75% quartiles, whiskers 5% and 95% quantiles and  
31 the asterisks the median of the data.

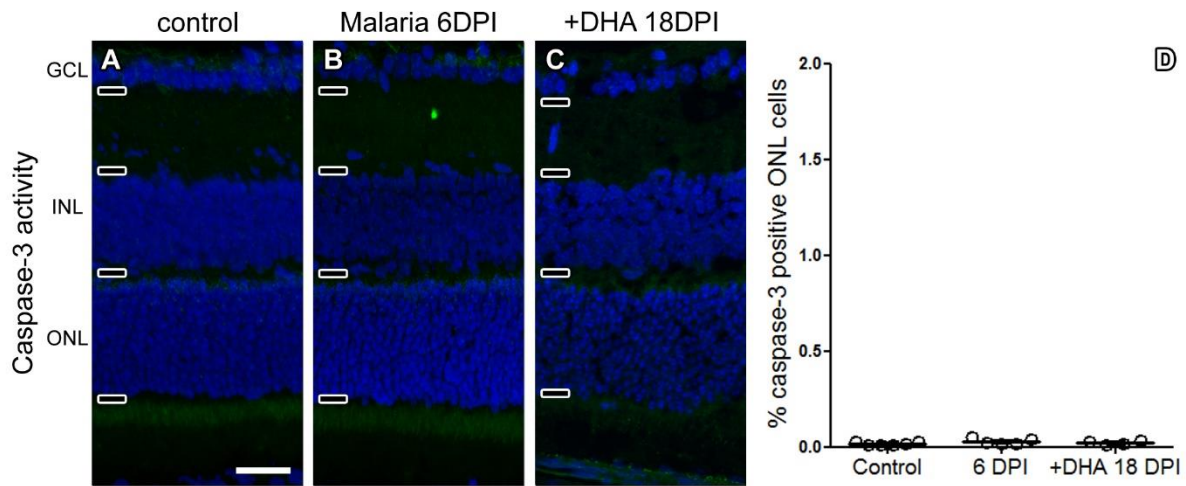
32



33

34 **Fig. S2: DHA treatment reduces parasitaemia and prevents further weight loss.** (A) After  
35 *P. berghei* infection, parasitaemia in the blood stream increased rapidly until the start of the  
36 DHA treatment at 6DPI. Afterwards, parasitaemia decreased until at 12DPI no parasites could  
37 be detected in blood. (B) The body weight of experimental animals decreased by about 8%  
38 until 6DPI. DHA treatment stabilized body weight till the end of the experiment. n = 11 animals  
39 (0DPI-6DPI), n = 4-5 animals (10DPI-18DPI).

40



41

42 **Fig. S3: Cell death in malarial retinopathy is independent of caspase activity.** *P. berghei*

43 infected mice presented with significantly increased numbers of dying, TUNEL positive cells at

44 6 and 18DPI (Figure 6). An immunostaining for activated caspase-3 did, however, not identify

45 any measurable increase of caspase activity at either time-point, indicating that malaria

46 induced neurodegeneration was caspase-independent and non-apoptotic. Scale bar in A = 50

47  $\mu\text{m}$ ; n (control) = 6 observations from 5 animals, n (6DPI) = 6/6; n (18DPI) = 4/4.

48

49

50

51

52

### **Captions for supplemental videos**

53

---

54 **Supplemental Video 1: Scanning laser ophthalmoscopy (SLO) reveals GFP-labelled**  
55 **parasites *in vivo*.** At 3DPI, mice infected with GFP-labelled *P. berghei* presented with  
56 fluorescence in non-invasive SLO imaging (*cf.* Fig. 2A). In the video, the GFP-label is visible  
57 travelling through the retinal vasculature. Note that the video is repeated twice, first in its  
58 original form, then with a red circle highlighting the vessel through which the GFP-label is  
59 moving. The video is representative for similar observations made in 11 different infected  
60 animals.

---

61

---

62 **Supplemental Video 2: Malaria-induced retinal layer aberrations are visible in optic**  
63 **coherence tomography (OCT).** At 3DPI, *P. berghei* infected mice were investigated using  
64 non-invasive *in vivo* OCT imaging. The video shows a volume scan through the infected retina  
65 superimposed on an SLO image (autofluorescent mode; *cf.* Fig 2A). Consecutive OCT scans  
66 are shown, going from inferior (I) towards superior (S), towards the optic nerve head. While  
67 large areas of the retina still display normal morphology (*cf.* Fig. 1 OCT), numerous alterations  
68 are visible as dark areas of variable size, sometimes leading to strong distortions of retinal  
69 layering. Such alterations are observed throughout the entire retina. Note that the video is  
70 repeated twice, first in its original form, then with red arrows indicating areas with obvious  
71 retinal layer alterations. The video is representative for similar observations made in 11  
72 different infected animals. The volume scan is orientated along the temporo (T) - nasal (N)  
73 axis.

---

74

75

76